

Contents lists available at ScienceDirect

# Petroleum Science

journal homepage: www.keaipublishing.com/en/journals/petroleum-science



# Original Paper

# Porosity prediction based on improved structural modeling deep learning method guided by petrophysical information



Bo-Cheng Tao  $^{a, b}$ , Huai-Lai Zhou  $^{a, b, c, *}$ , Wen-Yue Wu  $^d$ , Gan Zhang  $^d$ , Bing Liu  $^{a, b}$ , Xing-Ye Liu  $^{a, b, e}$ 

- a Key Lab of Earth Exploration and Information Techniques of Ministry of Education, Chengdu University of Technology, Chengdu, 610059, Sichuan, China
- <sup>b</sup> College of Geophysics, Chengdu University of Technology, Chengdu, 610059, Sichuan, China
- <sup>c</sup> State Key Laboratory of Oil and Gas Reservoir Geology and Exploitation, Chengdu University of Technology, Chengdu, 610059, Sichuan, China
- <sup>d</sup> Sichuan Water Development Investigation, Design and Research Co., Ltd, Chengdu, 610059, Sichuan, China
- e State Key Laboratory of Geohazard Prevention and Geoenvironment Protection, Chengdu University of Technology, Chengdu, 610059, Sichuan, China

#### ARTICLE INFO

# Article history: Received 1 August 2024 Received in revised form 21 December 2024 Accepted 24 March 2025 Available online 26 March 2025

Edited by Meng-Jiao Zhou

Keywords:
Porosity prediction
Deep learning
Improved structural modeling
Petrophysical information

# ABSTRACT

Porosity is an important attribute for evaluating the petrophysical properties of reservoirs, and has guiding significance for the exploration and development of oil and gas, The seismic inversion is a key method for comprehensively obtaining the porosity. Deep learning methods provide an intelligent approach to suppress the ambiguity of the conventional inversion method. However, under the trace-bytrace inversion strategy, there is a lack of constraints from geological structural information, resulting in poor lateral continuity of prediction results. In addition, the heterogeneity and the sedimentary variability of subsurface media also lead to uncertainty in intelligent prediction. To achieve fine prediction of porosity, we consider the lateral continuity and variability and propose an improved structural modeling deep learning porosity prediction method. First, we combine well data, waveform attributes, and structural information as constraints to model geophysical parameters, constructing a high-quality training dataset with sedimentary facies-controlled significance. Subsequently, we introduce a gated axial attention mechanism to enhance the features of dataset and design a bidirectional closed-loop network system constrained by inversion and forward processes. The constraint coefficient is adaptively adjusted by the petrophysical information contained between the porosity and impedance in the study area. We demonstrate the effectiveness of the adaptive coefficient through numerical experiments. Finally, we compare the performance differences between the proposed method and conventional deep learning methods using data from two study areas. The proposed method achieves better consistency with the logging porosity, demonstrating the superiority of the proposed method.

© 2025 The Authors. Publishing services by Elsevier B.V. on behalf of KeAi Communications Co. Ltd. This is an open access article under the CC BY-NC-ND license (http://creativecommons.org/licenses/by-nc-nd/

4.0/).

#### 1. Introduction

Porosity is related to the petrophysical properties, lithology, and fluid characteristics of underground media (Doyen, 1988; Bernabé, 1995; Wong et al., 1995; Mukerji et al., 2001b), and determines the favorable degree of reservoirs (Su et al., 2023). Fine prediction of porosity plays a crucial role in the beneficial development of oil and gas resources (Zheng et al., 2020; Liu et al., 2022; Yang et al., 2023). Porosity is typically obtained through core logging analysis and

However, significant uncertainties arise when extrapolating them to the lateral areas between wells (Han et al., 2022; Jin et al., 2024). Seismic inversion, on the other hand, infers the physical properties of geological media from observed seismic data (Aki and Richards, 2002). Seismic data provides abundant information about unexplored areas, enabling three-dimensional characterization of geological structures and comprehensive analysis of reservoirs and sedimentary environments (Aleardi et al., 2018; Das and Mukerji,

2020; Liu et al., 2022). Previous research indicates that the

seismic inversion. Core logging directly measures porosity using core data (Luffel and Guidry, 1992) or estimates it through a rockphysics model derived from well data (Avseth et al., 2010;

Johansen et al., 2013; Liu et al., 2015, 2020; Zhang et al., 2024).

\* Corresponding author. E-mail address: zhouhuailai06@cdut.edu.cn (H.-L. Zhou).

https://doi.org/10.1016/j.petsci.2025.03.035

seismic wave propagation velocity within a certain depth range is influenced by the porosity of the medium (Wyllie et al., 1956). Although seismic data cannot directly reveal porosity information, it exhibits an inherent physical correlation between wavefield reflection and petrophysical properties (Sang et al., 2023). Therefore, leveraging seismic data as an intermediary, the seismic inversion method has achieved a reasonable extrapolation of porosity from well sections to the underground space (Liu et al., 2023c), which represents the most comprehensive porosity prediction approach and provides important reference for further evaluating the petrophysical properties of reservoir (Gholami et al., 2022).

Seismic data referred to in seismic inversion methods encompasses a broad spectrum, including pre-stack seismic data (Zhang et al., 2017; Yang et al., 2023), post-stack seismic data (Figueiredo et al., 2017; Feng et al., 2020), and various seismic attributes (Fattahi and Karimpouli, 2016; Zou et al., 2021; Song et al., 2023). In addition, the implementation process of the inversion method varies significantly depending on the specific approach employed. A classic approach is to obtain elastic parameters through pre-stack or post-stack seismic data inversion, and then calculate porosity based on rock-physical relationships (Mukerji et al., 2001a; Adelinet and Ravalec, 2015; Pang et al., 2020; Ali et al., 2023). This process involves a multi-step process and carries the risk of accumulating errors (Han et al., 2022). Another classic approach is usually based on Bayesian inversion frameworks, ensuring consistency between petrophysical and elastic parameters, and achieving joint or synchronous inversion of petrophysical parameters (Bosch, 2004: Helgesen et al., 2000). The above methods adhere to the principles of geophysical inversion, and the accuracy of porosity inversion heavily depends on the reliability of inversion algorithms and physical models. Despite these theoretical foundations, the inversion process remains inherently uncertain and unstable (Lindseth, 1979; Shahraeeni et al., 2012). In addition, the seismic reflection mechanisms are highly complex and variable, with nonlinearity and multiplicity running through the entire process of seismic inversion (Das and Mukerji, 2020). These challenges complicate the porosity prediction using seismic data and hinder the precise evaluation of reservoir properties.

Deep learning methods provide a new way to achieve reservoir inversion and simulation (Das et al., 2019; Liu et al., 2022). Deep learning employs deep neural networks with powerful nonlinear expression capabilities. In theory, deep neural networks can establish complex nonlinear mapping relationships from observation data to any model data. By training a large number of labeled datasets, they can deeply mine the reservoir information contained in seismic data, effectively alleviating the nonlinear issue exhibited by conventional inversion methods (Das et al., 2019; Figueiredo et al., 2019; Zhang et al., 2022). In addition, an increasing number of studies have shown that implementing a dual scale constrained deep learning approach in inversion networks with external forward networks can reduce the dependency of neural networks on datasets (Alfarraj and AlRegib, 2019; Sun et al., 2019; Yuan et al., 2022), and has been widely applied in examples of intelligent prediction of porosity (Han et al., 2022; Sang et al., 2023).

In practices, porosity label data is derived from logging data, which is inherently one-dimensional and limited in quantity due to drilling cost. The "trace-by-trace" strategy is usually used to predict the overall data. However, this strategy overlooks the lateral correlation of seismic data, resulting in inadequate lateral continuity in prediction results (Yuan et al., 2015; Wu et al., 2021). Meanwhile, geological formations are highly heterogeneous and are affected by tectonic movements and sedimentation processes. The spatial distribution characteristics of geological bodies are extremely complex (Liu et al., 2023a). Based on discrete well data,

constructing an observation model of subsurface media poses a substantial challenge, as it is difficult to ensure the reliability of the model in areas with pronounced lateral variability.

The seismic horizon reflects geological structure information. A multi-trace algorithm constrained by horizon can obtain inversion results with high lateral continuity (Yuan et al., 2015; Liu et al., 2023b: Tao et al., 2024). In addition, from the perspective of sedimentology, seismic waveforms encapsulate seismic kinematic and dynamic characteristics, serving as comprehensive representations of geological information such as sedimentation, lithofacies combinations, reservoir properties, and fluids (Chen et al., 2020). Changes in seismic waveforms often reflect the changes in lithofacies combinations within the same stratum, which is a manifestation of sedimentary facies. As a result, similar sedimentary environments typically exhibit similar seismic waveform characteristics, and the lateral differences in seismic waveforms can effectively indicate changes in sedimentary facies in space (Chen et al., 2023). The modeling method based on seismic waveform attributes fully considers the spatial variability of strata. The constructed reservoir parameter model is driven by geological knowledge and laterally constrained by sedimentary facies, which could reduce the uncertainty of the model between wells (Huang et al., 2020).

In order to achieve fine porosity prediction, taking into account the spatial continuity and sedimentary variability of strata, we use seismic waveform and structural attributes for high-resolution modeling, and propose a deep learning porosity prediction method based on knowledge and data joint driven. Meanwhile, we introduce a gated axial attention mechanism and design a neural network for porosity inversion and seismic forward modeling to achieve bidirectional closed-loop deep learning. Moreover, we develop an adaptive loss function with dual scale constraints and analyze its impact on prediction performance. The proposed method is validated through two case studies involving buried hill data and shale reservoir data. Comparative analyses with conventional one-dimensional and two-dimensional deep learning methods highlight the superior prediction performance of the proposed method, providing an intelligent strategy for fine porosity prediction.

# 2. Method and theory

Our method aims to achieve fine porosity prediction. First, waveform-guided structural modeling is carried out through well data, seismic waveforms, and structural information to construct impedance and porosity models with sedimentary faciescontrolled significance. The impedance model is then used to synthesize fine seismic datasets. Subsequently, the seismic and porosity datasets serve as input and output, respectively, for training the proposed bidirectional closed-loop neural network. During this process, the weights of the forward network are adaptively fed back by the petrophysical crossplot analysis between porosity and impedance. After training, we can obtain the mapping relationship between seismic data and porosity. Finally, the real seismic data is input into the bidirectional network. The forward network and the inversion network then output the predicted seismic data and the predicted porosity respectively, based on the mapping relationship, thereby fulfilling the task of this article. The technical flowchart of the deep learning porosity prediction method proposed in this article is shown in Fig. 1.

The main contributions are summarized as follows.

(1) The training set constructed by the proposed method integrates structural information and seismic waveform attributes, which effectively considers the lateral continuity and

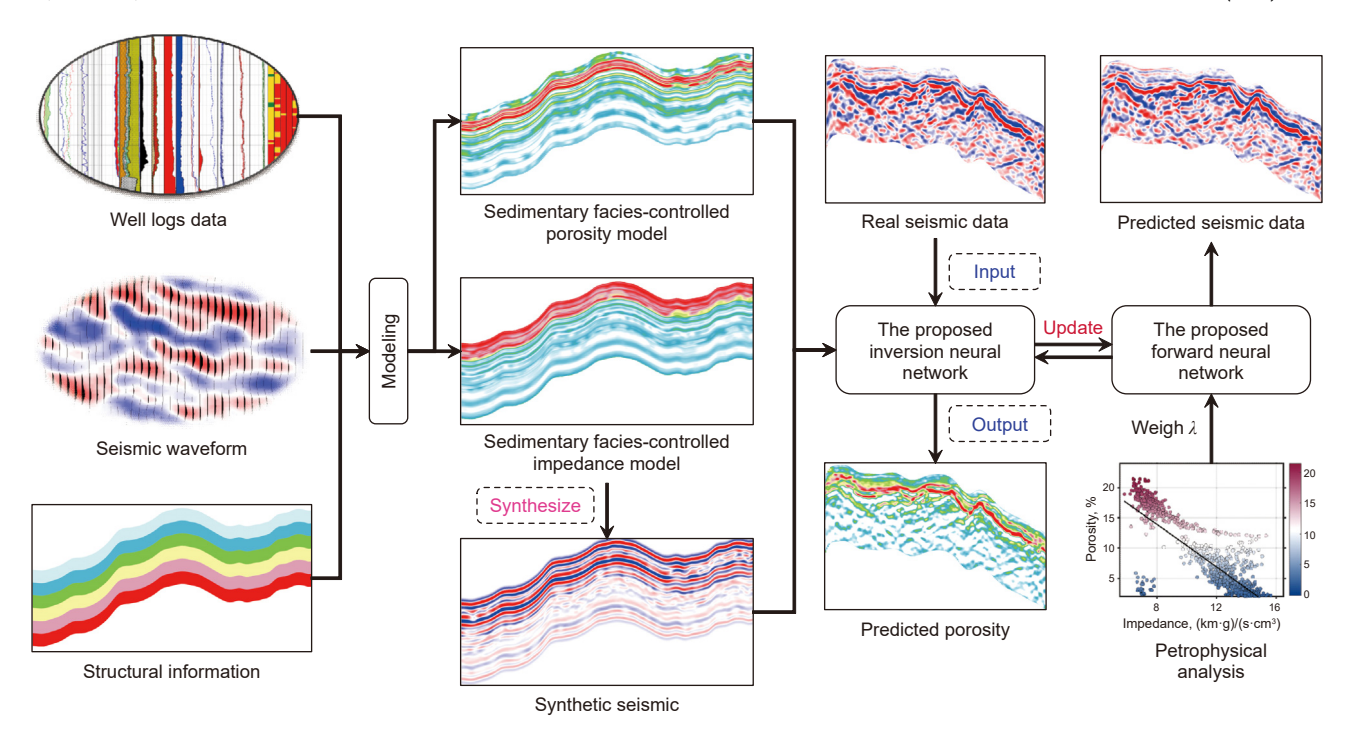


Fig. 1. The workflow of the proposed method.

- spatial variability of geological bodies during the training process, reducing the prediction uncertainty.
- (2) The designed bidirectional closed-loop neural network introduces a gated axial attention mechanism, which alleviates the dependency of deep learning on a large number of labeled samples.
- (3) Guided by the petrophysical information, the network adaptively balances the matching between input and output data during the training process, which helps the network learn more effective porosity features.

# 2.1. Improved structural modeling method

The construction of the training sample is the first step in the proposed method, providing a high-quality dataset foundation for deep learning. According to research (Chen et al., 2020), while different wells are in the same sedimentary stratum, their waveforms within well-nearby traces and logging curves have high similarity, so a mapping relationship between seismic waveforms and high-frequency logging curves can be established. Seismic waveform guided modeling refers to using the similarity of seismic waveforms as modeling principles, driving the simulation of broadband logging parameters between wells with sedimentary information, and achieving high-resolution reservoir parameter modeling. In the modeling process, there are two steps involved: seismic waveform clustering based on singular value decomposition and well frequency band information matching based on wavelet transform.

The mapping relationship between seismic waveforms and reservoir parameters of wells can be described in the following form:

$$\mathbf{A} = \mathbf{S} \Lambda \mathbf{W}^{\mathrm{T}} \tag{1}$$

where **S** represents seismic waveform data, which is a  $n \times n$  order orthogonal matrix; **W** represents the well parameters, which is a

 $m \times m$  order orthogonal matrix;  $\mathbf{W}^{\mathrm{T}}$  is its conjugate transpose;  $\mathbf{\Lambda}$  represents the correlation between seismic waveforms and well parameters, which is a  $n \times m$  order non negative diagonal matrix;  $\mathbf{A}$  represents the mapping relationship between waveform and well parameters, and is a  $n \times m$  order matrix.

Further utilize the Singular Value Decomposition (SVD) method to perform orthogonal decomposition on the matrix **A**, in order to achieve dynamic clustering of waveforms:

$$\mathbf{A} = \sum_{i=1}^{r} \delta_i \mathbf{s}_i \mathbf{w}_i^{\mathrm{T}}$$
 (2)

where i represents singular value; r represents the rank of the matrix  $\mathbf{A}$ ;  $\mathbf{s}_i$  is the i-th eigenvector of  $\mathbf{A}$ ;  $\mathbf{w}_i$  is the i-th eigenvector of  $\mathbf{A}^T$ ;  $\delta_i$  is the square root of the eigenvalue  $\mathbf{A}\mathbf{A}^T$ . So matrix  $\mathbf{A}$  can be decomposed into the algebraic sum of r eigenvectors, and its total energy can be expressed as

$$\|\mathbf{A}\|^2 = \sum_{i=1}^r \delta_i^2 \tag{3}$$

By using the singular vectors corresponding to the first r nonzero singular values to represent the main features of matrix  $\mathbf{A}$ , efficient dynamic clustering of seismic waveforms is achieved, thereby generating datasets of waveform and well parameter with different sedimentary characteristics. In addition, considering the mismatch between waveform data and logging data in the frequency band, frequency domain filtering is performed on the logging curves based on the discrete wavelet transform shown in Eq. (4) to extract the common structure of all logging curves in the datasets. This common structure is the macroscopic feature of logging parameters, which is a low to medium frequency filtering result compared to logging data. However, for seismic data, it is a high-resolution information:

$$O(l) = \arg(\min \|C - \overline{C}\|) = \arg\left(\min \left\| \int_0^l \varphi(w, t) dw - \overline{C} \right\| \right)$$
 (4)

where *l* is the cutoff frequency related to the common structure, *C* is the logging curve,  $\overline{C}$  is its mean, and  $\varphi(w,t)$  is the wavelet function.

Furthermore, we use structural information as a framework constraint and interpolate common structures along the horizon to construct high quality facies-controlled porosity model and impedance model. The porosity model will be used to construct the labeled dataset, which is the learning objective of this article, while the impedance model will be used for further seismic modeling. The seismic modeling follows the same process as post-stack forward modeling (Russell, 1988). The impedance  $Z_p$  can be expressed as the product of the dielectric density  $\rho$  and velocity  $\nu$ :

$$Z_{\mathbf{p}}(t_i) = \rho(t_i) \cdot v(t_i) \tag{5}$$

where  $t_i (i=1,2,...,n+1)$  represents the depth of two-way travel for the i-th discrete grid. According to the theory of elastic waves, in the case of vertical incidence of plane waves, the impedance determines the reflection coefficient of the geological interface:

$$R(t_i) = \frac{Z_p(t_{i+1}) - Z_p(t_i)}{Z_p(t_{i+1}) + Z_p(t_i)}$$
(6)

By using convolution theory, the simulated seismic wavelet W and calculated reflection coefficient R according to Eq. (6) are convolved to synthesize the seismic model  $S_{\text{model}}$ :

$$S_{\text{model}}(t) = \sum_{i=1}^{n} R(t_i) \cdot W(t - t_i) = R(t) * W(t)$$
 (7)

The porosity model and synthetic seismic model using constraints of structure and waveform information integrates multisource geological information and has facies-controlled significance, and this modeling method is named the improved structural modeling (ISM) method in this article.

# 2.2. Gated axial attention mechanism

The quality and quantity of the training set are important factors that affect the training effectiveness. When there is limited training data, deep learning models are difficult to demonstrate good performance. In practice, drilling data is usually expensive and scarce, and a small number of well samples is a huge challenge for building a training set to deep learning. How to achieve effective deep learning with few samples? To address this, we introduce a gated axial attention (GAA) mechanism model (Valanarasu et al., 2021).

Unlike the self-attention mechanism, the axial attention mechanism performs attention calculations along the height and width axes of the feature map, simulating the self-attention mechanism through axial encoding coverage. This greatly reduces the complexity of attention calculations and enables the axial attention model to obtain information more efficiently. Meanwhile, positional encoding information is an important concept in attention mechanisms and is crucial for modeling long-range dependencies. The axial attention mechanism introduces a positional encoding bias term, namely relative positional encoding, which makes the mechanism more sensitive to positional encoding. Finally, in order to make the training applicable to a limited dataset, we introduce a gated mechanism G for relative position encoding. If the relative position encoding is accurately learned, the corresponding gated weight should be higher, and vice versa, in order to improve the accuracy of encoding information learning. The gated

axial attention layer is shown in Fig. 2. For a given input feature map x, the attention calculation along the width axis can be expressed as

$$y_{ij} = \sum_{w=1}^{W} \text{Softmax} \left( q_T^{ij} k_{iw} + G_Q q_{ij}^{T} r_{iw}^{Q} + G_K k_{iw}^{T} r_{iw}^{K} \right) \left( \nu_{iw} + G_V r_{iw}^{V} \right)$$
(8

where the input feature map x passes through the weight matrices  $\mathbf{W}_{\mathrm{Q}}$ ,  $\mathbf{W}_{\mathrm{K}}$ , and  $\mathbf{W}_{\mathrm{V}}$  to generate the  $q_{T}^{ij}$  (query),  $k_{iw}^{\mathrm{T}}$  (key), and  $v_{iw}$  (value) in Eq. (8), which are all linear projections of x.  $r_{iw}^{\mathrm{Q}}$ ,  $r_{iw}^{\mathrm{K}}$ , and  $r_{iw}^{\mathrm{V}}$  are all learnable relative position codes, while  $G_{\mathrm{Q}}$ ,  $G_{\mathrm{K}}$ , and  $G_{\mathrm{V}}$  are learnable gated factors that control the impact of the learned relative position codes on the encoding context. We initialize gated factors as 0.1, and after matrix multiplication, addition, and softmax activation operations as shown in Fig. 2, we obtain the output feature map y. Similarly, the attention calculation along the height axis is also consistent with the above process.

#### 2.3. The bidirectional closed-loop network

This article constructs a high-quality sample set through the ISM method and introduces the GAA mechanism for feature enhancement. Another key to the success of deep learning is a targeted neural network. In network training, the training data will be projected onto a high-dimensional information space, and a neural network that matches the task can efficiently and accurately extract feature information from it. Our work is essentially a data regression task, and examples of using neural networks to predict geophysical parameters are not uncommon, among which convolutional neural network (CNN) is the most classic example. CNN has the ability of local perception, enabling precise encoding of local detail information. Meanwhile, CNN benefits from the property of kernel sharing, which allows for efficient dimensionality reduction when processing large amounts of seismic data.

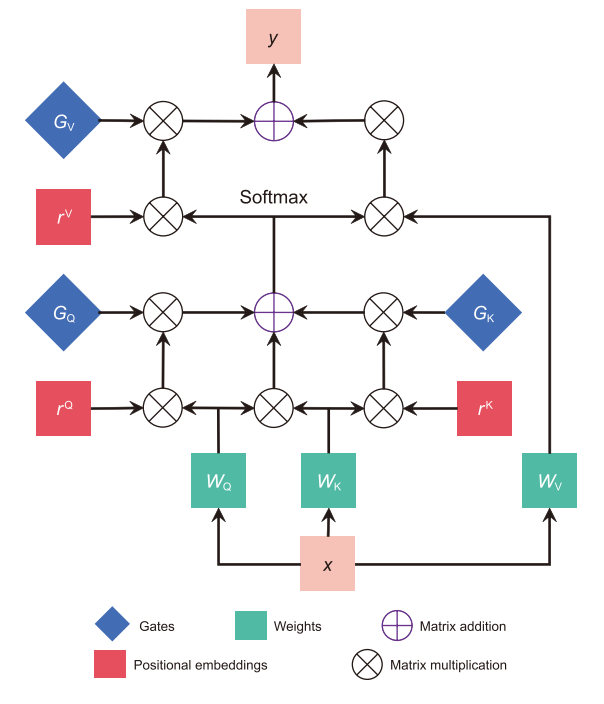


Fig. 2. Gated axial attention layer, which is a basic module for calculating attention along the width and height axes.

However, CNN has the drawback of fixed convolution kernels, and mismatched convolution kernels may lead to incomplete extraction of data features by the network.

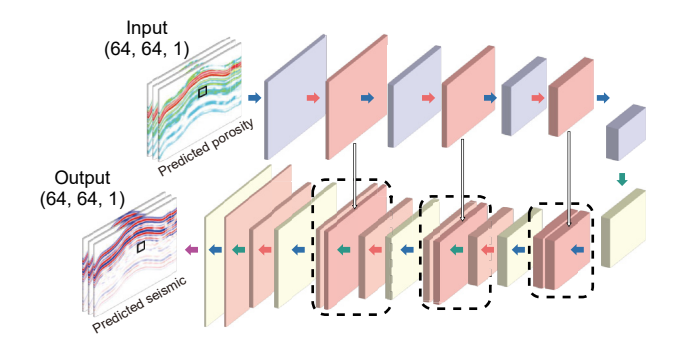
The prediction of reservoir parameters is a systematic and comprehensive process, and relying solely on local data encoding may lead to significant uncertainty. Within the same stratum, under the influence of compaction and tectonic movements, reservoir parameters have inherent physical correlations in the vertical direction, representing the whole sedimentary trend. Therefore, long-range dependencies during training are crucial, which can reflect the sedimentary characteristics of the strata at a macro level. On this basis, Transformer networks have emerged (Vaswani et al., 2017), which interact and transmit information through attention mechanisms, achieving effective long-range relationship modeling. This makes training guided by global vertical information (stratigraphic sedimentary trends), effectively solving the problem of lack of macroscopic stratigraphic information in prediction results. However, the representation of classic Transformer networks is one-dimensional, and the network cannot capture local details horizontally, resulting in a lack of constraints on spatial structure and sedimentary details during training, making it difficult to achieve fine prediction of reservoir parameters.

Based on the above considerations, this article introduces a TransUNet network structure (Chen et al., 2021) that combines the characteristics of CNN and Transformer and expands the network dimension, and proposes a porosity inversion neural network based on Fig. 3(a). The seismic data is encoded and decoded by the network to obtain the predicted porosity, and the training process is carried out in the form of data patches. In encoding, seismic data is extracted through three initial convolutional layers equipped with GAA modules for shallow feature collection. Each GAA module consists of a normalization layer, a gated multi-head attention module calculated along the height axis, a gated multi-head attention module calculated along the width axis, and a feature combination layer. Each gated multi-head attention module has 8 gated attention layers as shown in Fig. 2. On this basis, the collected shallow features such as structural and sedimentary information are projected into Transformer layers as shown in Fig. 3(b). The Transformer encoder implemented in this article mainly consists of multi-head self-attention layers (MSA), multi-layer perception (MLP), layer normalization (LayerNorm), and residual connections. The overall architecture is based on the classic Transformer model (Vaswani et al., 2017), and the output of each encoder module will serve as the input for the next module. In the specific configuration, we set the attention head of MSA to 4, the hidden dimension of MLP to 2048 and the number of transformer layers to 12. The Transformer layers deeply mine the petrophysical property information of labeled data, thus implementing the encoding process of features. During the decoding process, deep communication involves reshaping and convolution to restore the shape before entering the Transformer layers. Then, the feature data is reconstructed through three progressive upsampling, convolution, and GAA module operations. Skip connections are used to combine the upsampled features with different high-resolution CNN features in the encoding, achieving accurate localization of petrophysical property information. Finally, the porosity results are output through a set of upsampling and two consecutive convolutional layers. The proposed inversion network takes into account both the long-range dependence of information, namely the sedimentary patterns of petrophysical properties in vertical space, and local details, such as lateral structural information, which helps to construct accurate encoding and decoding relationships.

In addition, we refer to the generalized seismic inversion and forward process, and construct a porosity-seismic forward network to achieve bidirectional closed-loop learning, reducing dependence on labeled datasets by simulating geophysical processes. As shown in Fig. 4, in order to accelerate computational efficiency and reduce task complexity, the forward network abandons the Transformer layer and retains the same structure as the inversion network for the remaining units. We used the Mish function (Misra, 2019) as a non-linear activation for all convolutional layers, and the output convolutional layer used a 1  $\times$  1 kernel. In addition, the other convolutional layers used a 3  $\times$  3 kernel.

# 2.4. Adaptive bidirectional constrain loss function

The proposed inversion network  $\Theta_1$  and forward network  $\Theta_2$  form a bidirectional conductive and closed-loop network system. The objective function of network training is jointly constrained by



 $\textbf{Fig. 4.} \ \ \textbf{The proposed forward neural network.} \ \ \textbf{The legend is the same as Fig. 2.}$ 

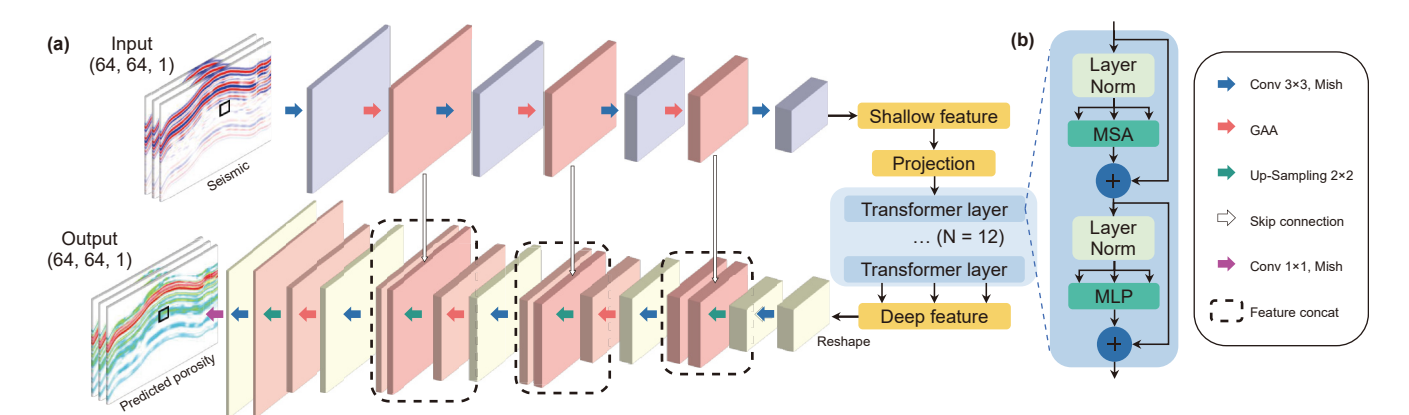


Fig. 3. The proposed inversion neural network: (a) the network architecture, (b) the schematic of the transformer layer.

inversion error and forward error, which can be expressed formally as

$$\mathcal{L}_{Bi} = \mathcal{L}_{\Theta_1} + \lambda \mathcal{L}_{\Theta_2} \tag{9}$$

where  $\mathscr{L}_{\Theta_1}$  represents the training loss of the porosity inversion network,  $\mathscr{L}_{\Theta_2}$  represents the training loss of the seismic forward network, and  $\mathscr{L}_{\mathrm{Bi}}$  represents the weighted bidirectional loss.  $\lambda$  is the weight coefficient of the forward network, which balances the matching between seismic data and target parameters. If the correlation between seismic data and target parameters is high, then the network should focus more on the prediction process of target parameters and reduce forward weights. On the contrary, if the correlation is low, the forward weight should be appropriately increased to strengthen the bidirectional constraint to alleviate this complex nonlinear problem and reduce the uncertainty of network prediction.

We measure the training loss of the network using mean squared error (MSE) and construct a training form suitable for the multi-source geological information training set in this article. Eq. (9) can be specifically represented as

$$\mathcal{L}_{Bi} = \frac{1}{NM} \sum_{i=1}^{N} \sum_{j=1}^{M} \left\{ \underbrace{\|\phi(i,j) - \Theta_{1}(s(i,j))\|_{2}^{2}}_{\mathcal{L}_{\Theta_{1}}} + \lambda \underbrace{\|s(i,j) - \Theta_{2}(\Theta_{1}(s(i,j)))\|_{2}^{2}}_{\mathcal{L}_{\Theta_{2}}} \right\}$$
(10)

where *N* and *M* represent the number of samples in both vertical and horizontal directions, s represents seismic data,  $\phi$  represents target data, i.e. porosity,  $\Theta_1(s)$  represents porosity predicted from s through inversion network, and  $\Theta_2(\Theta_1(s))$  represents seismic data further synthesized from predicted porosity. Another key to the objective function is to set the weight coefficients  $\lambda$ . Our task is to establish a high-precision mapping relationship between seismic data and porosity. Seismic data characterizes the reflection of the strata, which is the convolution result of reflection coefficient and seismic wavelet. The reflection coefficient of the strata is determined by the difference in impedance between the upper and lower media. Therefore, fundamentally speaking, our study can trace the inherent physical correlation between impedance and porosity. If the negative correlation between impedance and porosity is high in the well data of the study area, a lower  $\lambda$  should be set, and vice versa. Meanwhile, the principle of inversion network as the main body should be followed, so  $\lambda \in [0, 1]$  can be quantitatively expressed as

$$\lambda = 1 - \alpha \tag{11}$$

where  $\alpha$  represents the negative correlation between impedance and porosity in logging data. When  $\alpha=1$ , it indicates that there is a complete negative correlation between impedance and porosity. Therefore, the task of this article can also be regarded as an approximate post-stack impedance solving problem. The determination of weight coefficients is guided by petrophysical information, serving as a regularization coefficient that adapts to the elastic-petrophysical property relationship. This makes it easier for the network to fit the petrophysical characteristics contained in seismic data, further enhancing the interpretability of deep learning models.

#### 3. Examples and results

In order to verify the effectiveness of the proposed method, we show examples of two different types of reservoirs in this section. Commonly used deep learning methods are introduced for comparison to demonstrate the advantages of the proposed method. In addition, we test several groups of weight coefficients  $\lambda$  and demonstrate the performance of adaptive coefficients guided by petrophysical information.

# 3.1. The study area A: a buried hill reservoir example

The study area A is located in southern China, and its typical seismic data is shown in Fig. 5. The exploration objective is a Mesozoic buried hill structure, and Well A1 is an important geological structure well deployed at the high-position buried hill interface. Geological experts mark favorable horizon as T1, which is a lithological boundary. The target horizon for this case study is the clastic rock strata that extends upwards for 100 ms and the granite strata that extends downwards for 300 ms in T1. The clastic rock strata marked by T1 horizon have high porosity characteristics due to weathering, strong seismic response, moderate continuity, and great exploration and development potential. The strata below T1 horizon represent the interior of the buried hill. The impedance of this strata increases, while the porosity decreases rapidly. However, there are also intersecting fracture systems developed, which still have certain exploration potential. The seismic reflection within the granite strata is of medium-high amplitude, with chaotic reflection characteristics and poor continuity. Therefore, the conventional structural modeling (SM) method struggles to achieve the required lateral accuracy, resulting in cumulative inversion errors.

We conduct ISM method using seismic and horizon data from three other wells in study area A (A1 well not involve in modeling). A waveform-guided impedance model and porosity model are constructed. Impedance model will be used to calculate the reflection coefficient and convolve with statistical wavelets extracted from study area to synthesize a seismic dataset. To demonstrate the differences between the ISM method and the conventional SM method, we present the modeling results of three random profiles using different methods. As shown in Fig. 6, the training datasets constructed by both modeling methods reflect complex structural information, and the models also exhibit sedimentary trends consistent with the area vertically, highlighting the high porosity characteristics of the T1 horizon. However, the model constructed by the ISM method exhibits lateral variability and has sedimentary facies-controlled significance. The synthesized seismic data (Fig. 6(c)) also has better matching with real situation. We ultimately randomly select modeled results from 5 profiles as the training dataset for the task, and perform data segmentation with a patch size of  $64 \times 64$  and a step size of (8, 8). Although our

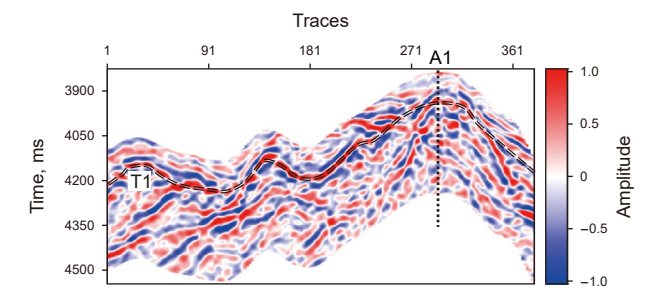


Fig. 5. The seismic data of study area A. The vertical black dotted line represents the trajectory of well A1 and the black double dotted line represents the horizon line T1.

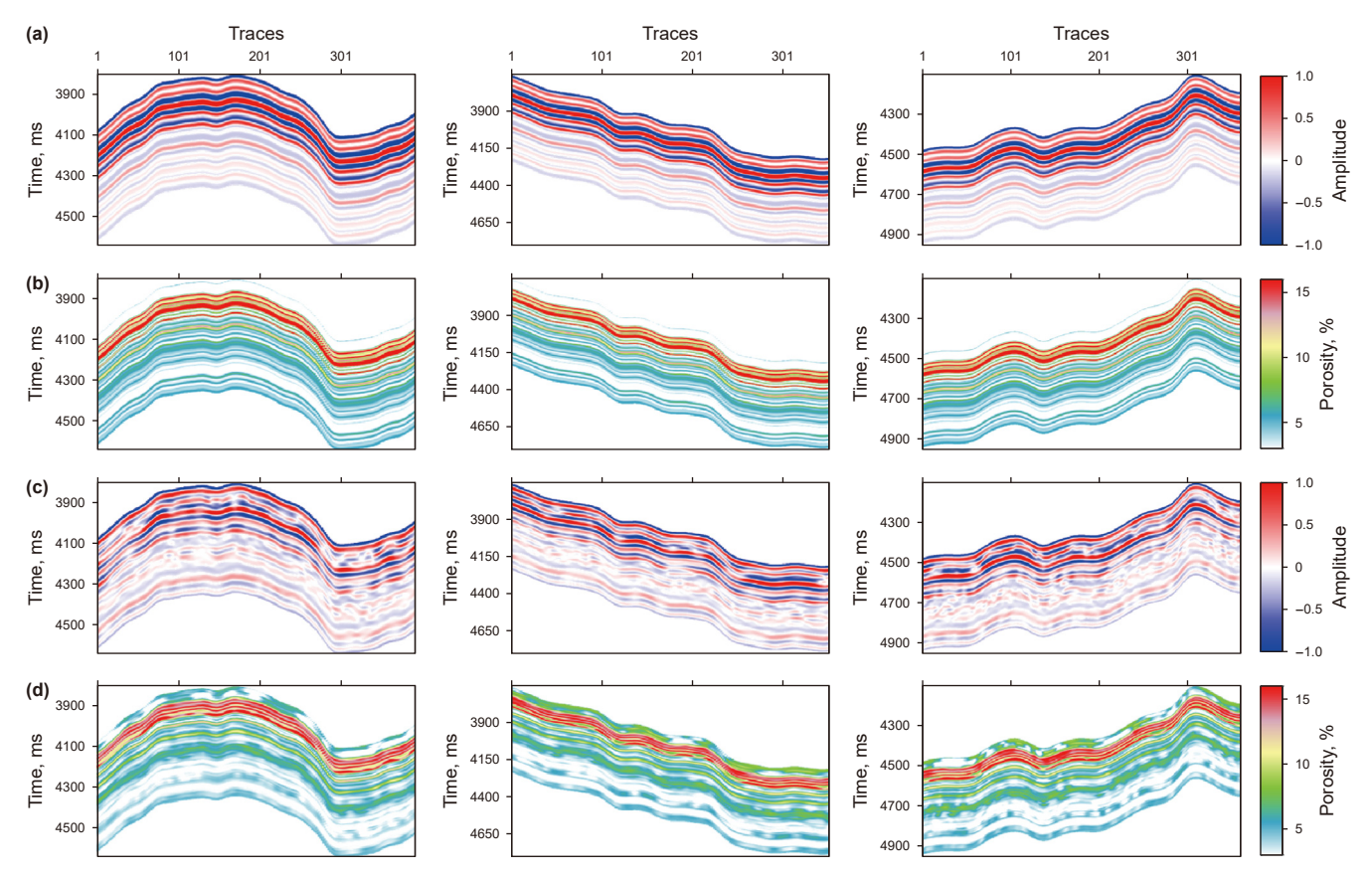
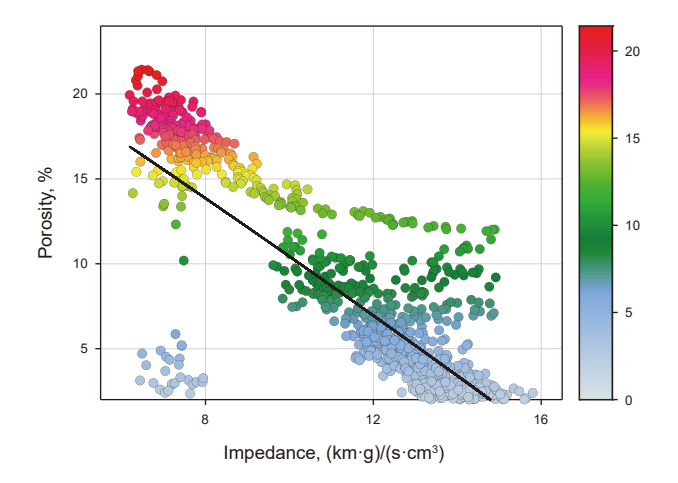


Fig. 6. Modeling results of study area A. The SM method constructed (a) seismic and (b) porosity dataset. The ISM method constructed (c) seismic and (d) porosity dataset. Each column result from the same profile.

task is in a small sample scenario, there is no need for additional data augmentation work due to the unique geological significance of the constructed training dataset. After removing invalid samples, a total of  $2\times24156\times64\times64$  training patches are obtained.

After constructing the training set, it is necessary to further focus on the network training strategy. For designing a closed-loop network, clarifying the regularization coefficients  $\lambda$  and constructing a highly adaptive objective function are significant steps. We conduct petrophysical crossplot analysis based on well A1 to explore the inherent relationship between the impedance and porosity within the target horizon of the study area. The crossplot result is shown in Fig. 7, which showcases that there is an overall negative correlation between the two attributes, but there is a certain degree of deviation of the data points on the black fitting line. The negative correlation between porosity and impedance is not high, only 0.583. According to Eq. (8),  $\lambda$  will be set to 0.417.

Based on the  $\lambda$  and the constructed training dataset, the ratio of the training and testing sets is 5:1. Further adjusting the hyperparameters of the network, we set the network learning rate to 0.001, the optimization algorithm to Adam, the batch size to 128, and 200 epochs. The porosity model modeled using ISM method is used as the training output, and the corresponding seismic model is used as the training input. The designed closed-loop network is used for iterative training. The loss during the training process is shown in Fig. 8, and we distinguish different networks and training validation modes to demonstrate this process. It can be seen that the training losses of both the inversion network and the forward network decrease rapidly. The inversion loss is generally lower than the forward loss, but some oscillations in the loss values are observed. These fluctuations can be attributed to the incomplete



**Fig. 7.** Petrophysical crossplot between porosity and impedance of A1 well, the formula of the black fitting line is  $\phi = -0.0022Z_p^2 - 1.7111Z_p + 27.7503$ , and the color of each point denotes its porosity value.

matching between the petrophysical and elastic properties in the study area. The network needs to use gradient descent to adapt to the complex mapping relationship between these attributes. However, porosity and seismic data are essentially characterized from different perspectives for the same geological body, and their similar response characteristics and physical correlations are inherent. Therefore, this relationship can be captured by training the network. The total training loss and validation set loss jointly constructed based on inversion loss and forward loss are shown in

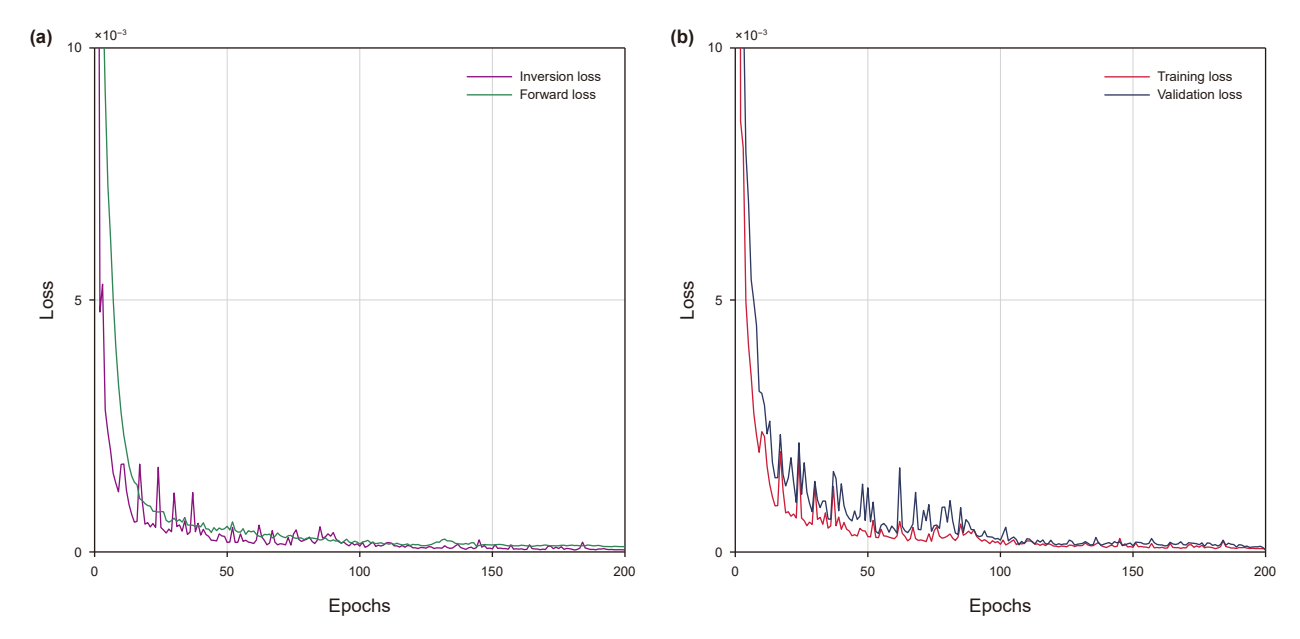


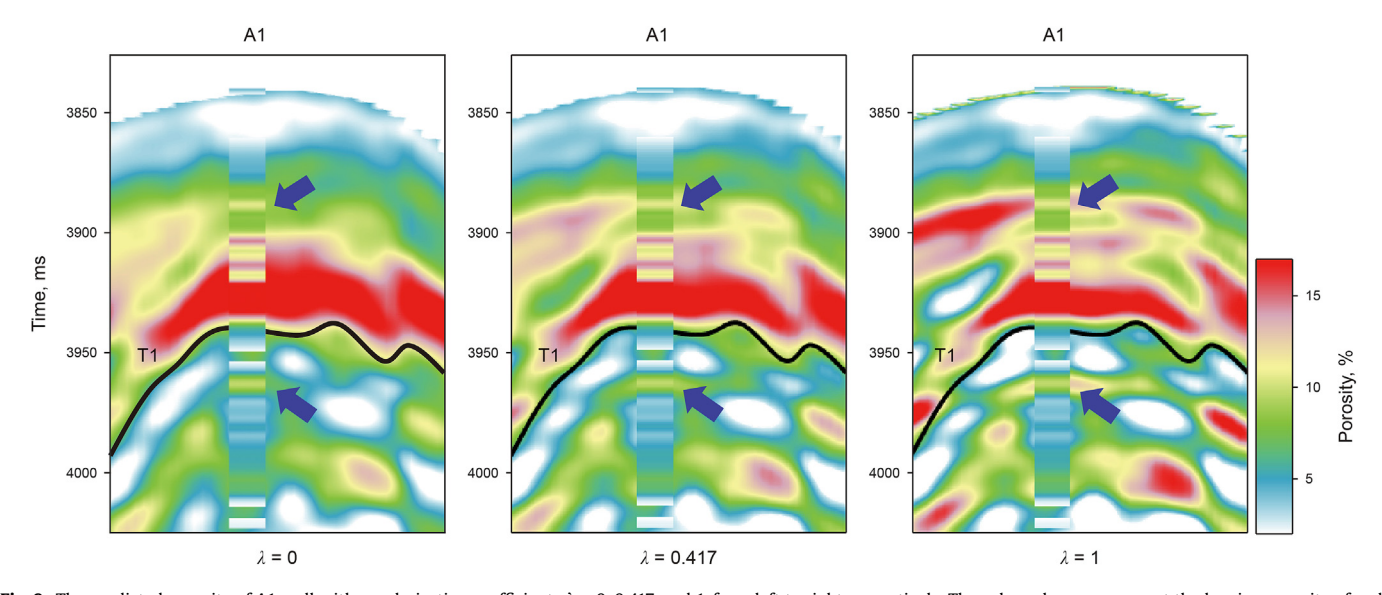
Fig. 8. Training loss of dataset from study area A. (a) Separate network loss, and (b) training and validation loss,

Fig. 8(b), which effectively reduces and tends to be stable. It can be considered that the network has learned the correct porosity features, and the trained model can be used for subsequent testing.

We test the effect of different forward network weights on the learning and prediction performance of ISM method, as shown in Fig. 9. We showcase the predicted porosity of well A1 nearby traces, with three sets of parameters from left to right:  $\lambda = 0$ ,  $\lambda = 0.417$ , and  $\lambda = 1$ . When  $\lambda = 0$ , the network lacks the constraints of the forward modeling process, leading to a lower level of precision in result and a more severe chunking effect on the profile; when  $\lambda = 0.417$ , introducing forward constraints alleviates the chunking effect and optimizes the correspondence between the thin layer indicated by the blue arrow and the well data; when  $\lambda = 1$ , the identifiable detail information of the profile significantly increases. We further conduct the error analysis shown in Fig. 10. Fig. 10(a) shows the crossplot of predicted porosity and logging porosity. It can be seen

that the deviation between the prediction results guided by petrophysical information ( $\lambda=0.417$ ) and the ground truth is the smallest, and almost all inversion sample points are concentrated within an absolute error range of  $\pm 2$ . Fig. 10(b) further summarizes the error histograms of different network parameters, verifying the above conclusion that the sample points with a normal distribution of  $\lambda=0.417$  are within the low error interval. After testing, we believe that higher weights help optimize the fineness of the results, but guided by the petrophysical information contained in impedance-porosity, the matching with well information is better.

After validating the effectiveness of forward weighting, we utilize ISM learning to achieve porosity prediction for the seismic data shown in Fig. 5. To compare the performance of different deep learning methods, we introduce the results of one-dimensional network learning (1D learning) and two-dimensional network structural modeling learning (SM learning). Fig. 11(a)—(c) show the



**Fig. 9.** The predicted porosity of A1 well with regularization coefficients  $\lambda = 0$ , 0.417, and 1, from left to right respectively. The color columns represent the logging porosity of well A1.

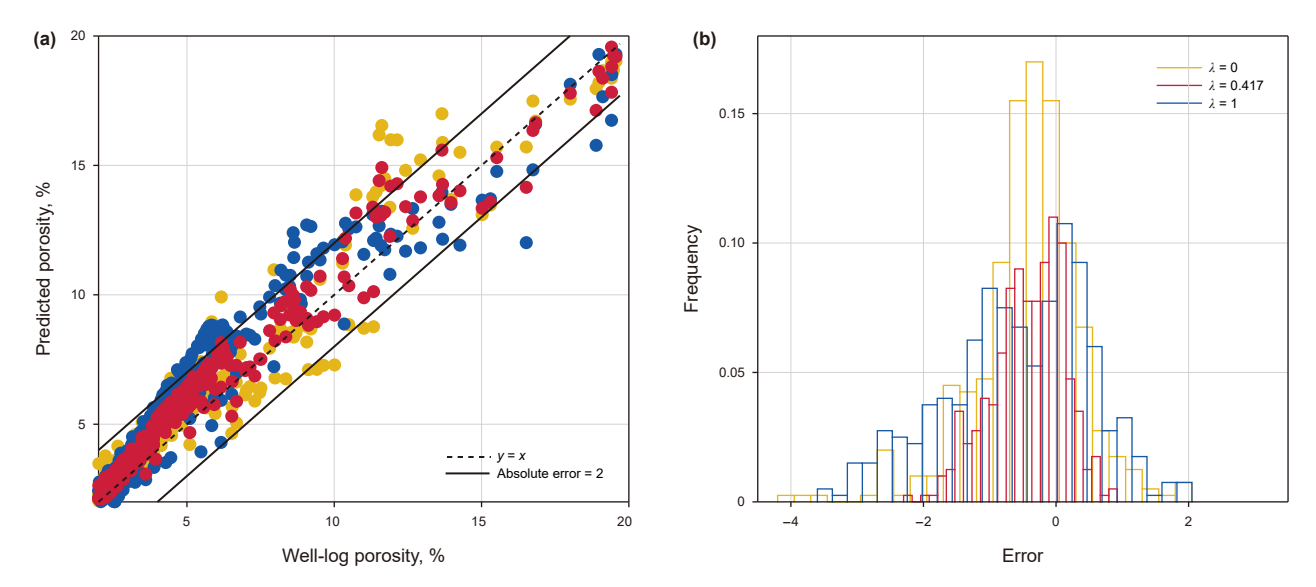


**Fig. 10.** Error analysis with different regularization coefficients. **(a)** Crossplot of predicted and true porosity; **(b)** error histogram. The yellow, red, and blue in the figure represent situations where  $\lambda = 0.0417$ , and 1.

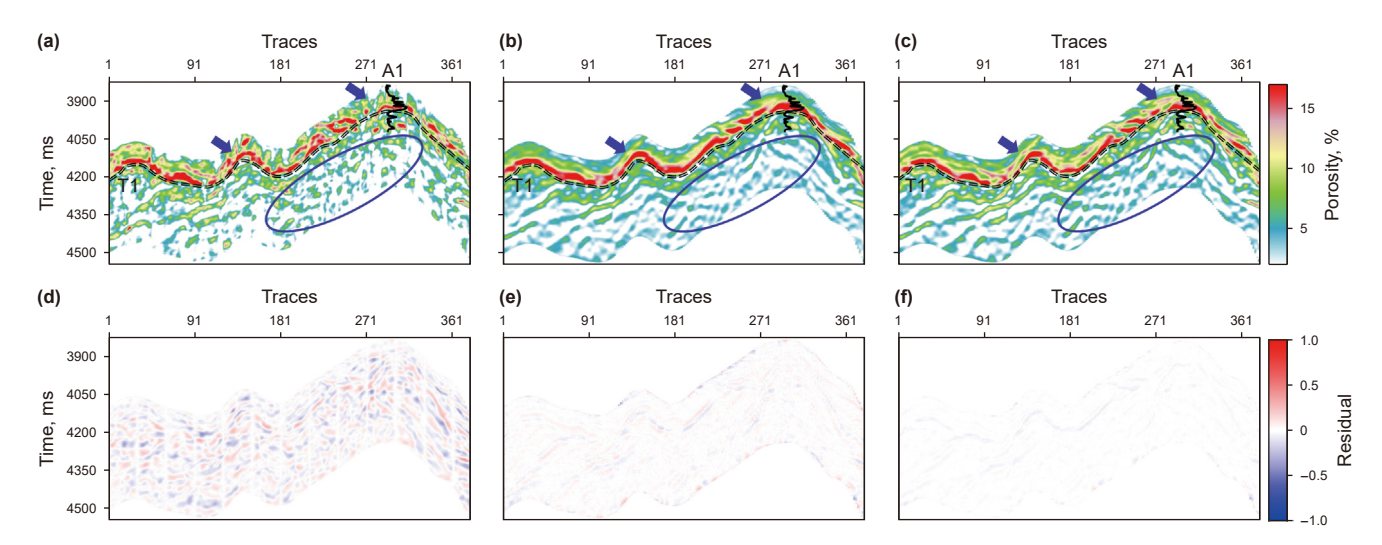


Fig. 11. Prediction results of seismic data cross well A1 in study area A based on different methods. Predicted porosity of (a) 1D learning, (b) SM learning and (c) ISM learning, the projected black curves represent logging porosity. The residual between real seismic data and synthetic seismic data of (d) 1D learning, (e) SM learning and (f) ISM learning.

predicted porosity of the above methods. The prediction results of the study area A through the three methods are in line with practical understanding and have a certain correspondence with the projected porosity curve. The predicted porosity using the 1D learning method is shown in Fig. 11(a). Unlike the two-dimensional network, the one-dimensional algorithm only establishes the mapping relationship between the well nearby seismic trace and the logging porosity. However, the overall prediction results are relatively fragmented, and the structural details of the interior are not continuous due to algorithm limitations. As indicated by the blue box in the figure, there are many vertical artifacts caused by the algorithm; Fig. 11(b) shows the predicted porosity based on SM learning, which effectively improves the lateral continuity of the results; Fig. 11(c) shows the predicted porosity of ISM learning, which further optimizes spatial variability while maintaining good lateral continuity, as indicated by the blue arrow, highlighting more detailed information. In addition, we also demonstrate the residuals between the synthetic seismic data and the real seismic

data using the above method. As shown in Fig. 11(d), the 1D learning method has a more significant residual, confirming its weak adaptability to chaotic reflections. In contrast, the residuals generated by two-dimensional algorithms are relatively small, while the residuals of ISM learning are weaker, indicating that introducing waveform constraints helps the network learn more accurate elastic-petrophysical property transformation relationships.

We compare the predicted porosity and true logging porosity of the well A1 nearby trace, as shown in Fig. 12. It can be seen that the 1D learning method exhibits large fluctuation in the prediction results, which shows a significant deviation from the true porosity. However, the SM learning and ISM learning methods achieve better alignment with the true porosity, maintaining consistency in the trend. Therefore, in order to quantitatively evaluate the prediction performance of different methods, we further calculate the Pearson correlation coefficient (PCC) and MSE between the well A1 nearby properties and the true porosity. The results, summarized in Table 1,

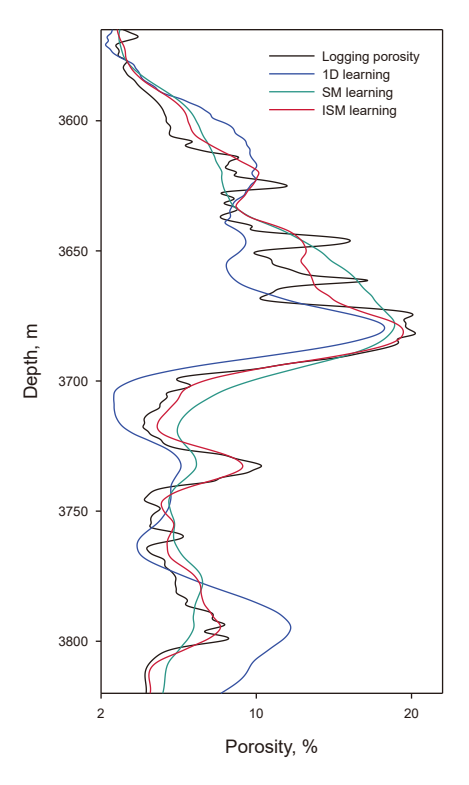


Fig. 12. Comparison of the prediction results of the well A1.

**Table 1** Prediction performance of well A1.

Metrics	Learning method				
	1D	SM	ISM		
PCC MSE	0.8313 0.0261	0.9032 0.0116	0.9225 0.0037		

the PCC calculated based on ISM learning is higher, reaching 0.9225, indicating better matching with well data. Furthermore, the MSE index confirms that the deviation between this method and the true porosity is also minimal, indicating the practicality and superiority of the ISM learning method in predicting porosity in study area A.

# 3.2. The study area B: a shale reservoir example

We further extend the proposed method to a shale reservoir research area to explore its feasibility for unconventional

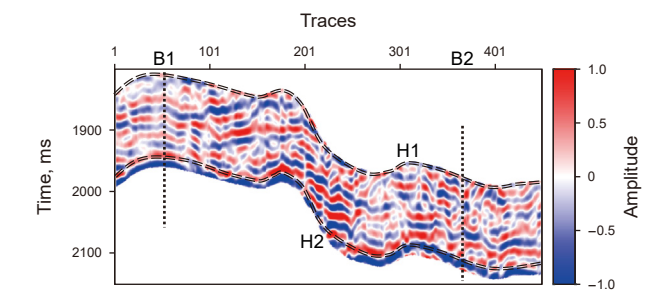


**Fig. 13.** The seismic data of study area B. The vertical black dotted lines represent the trajectory of wells B1 and B2 and the black double dotted lines represent the H1 and H2 horizon lines.

reservoirs. Study area B is located in the Sichuan Basin in southwestern China, and its seismic survey covers four wells. Fig. 13 shows the seismic profiles crossing wells B1 and B2 in the area, with the stratigraphic layers between horizon lines H1 and H2 being the target horizon for this study. The main lithology of the target horizon is black gray shale. The overlying strata of the H2 horizon are considered as a continuous favorable gas layer with a relatively stable thickness, generally between 44 and 72 m, and have high porosity and high TOC logging response characteristics. The logging interpretation suggests that the favorable degree of the reservoir in this area is highly correlated with porosity, therefore the fine prediction of porosity have significant guiding significance for the beneficial development of shale reservoirs in this area.

We use impedance and porosity data from two wells in study area B, except for B1 and B2, as well as seismic horizons, to conduct training set modeling for the SM method. As shown in Fig. 14(a) and (b), the modeling results of seismic and porosity of three profiles are randomly displayed. The results reflect the structural characteristics of the area and the vertical sedimentary state of petrophysical properties. The essence of two-dimensional deep learning methods is still to establish the relationship between elastic and petrophysical properties of wells, and then expand well data from one-dimensional space to multi-dimensional space by structural information. Its lateral variability mainly depends on well data. Therefore, the lateral differences in SM modeling results are not significant, and the issue of modelization is severe, which does not match the real situation. In contrast, the seismic and porosity datasets modeled by the ISM method are shown in Fig. 14(c) and (d). After adding constraints of waveform information, the lateral variability of the model is further reflected. At this point, the model has sedimentary facies-controlled significance and better fit with real seismic data, which is beneficial for the network to learn more accurate porosity features.

We analyze the negative correlation between impedance and porosity based on well data from study area B, and determine the weights of the forward network. As shown in Fig. 15, there is a quadratic negative correlation of impedance and porosity in this area. The negative correlation  $\alpha$  between logging data and the fitted nonlinear formula is 0.764, which  $\lambda$  will be further set to 0.236. We randomly divide the training set and validation set in a 5:1 ratio, and set 200 epochs for network training. The loss changes of the forward and inversion networks, as well as the training and validation sets, are shown in Fig. 16. Although some oscillations in the loss value are observed during the training process, it is gradually decreasing and tends to a stable low value after 150 epochs, indicating the effectiveness of the training.

Based on the trained model, porosity prediction of seismic data from wells B1 and B2 is carried out, and the spatial distribution of favorable gas layers is explored, as shown in Fig. 17(c). Meanwhile, we compare and demonstrate the predicted porosity using 1D learning and SM learning, as shown in Fig. 17(a) and (b). Three deep learning prediction methods have effectively identified favorable shale gas layers at the H2 horizon, aligning with existing geological knowledge as a whole. However, one-dimensional algorithm struggles to adapt to the structural variability of undulating strata, so some discontinuous vertical bar shaped artifacts appear at the blue box markings in the figure. These artifacts caused by the algorithm mechanism will further interfere with subsequent reservoir interpretation. The SM learning improves the lateral continuity of the prediction results, but overestimates the favorableness of reservoirs at the blue arrow markings, which contradicts the logging conclusion. In contrast, the ISM learning results that introduce constraint of waveform attribute into the training set accurately capture the vertical petrophysical properties and sedimentation patterns of the strata, while achieving more precise porosity

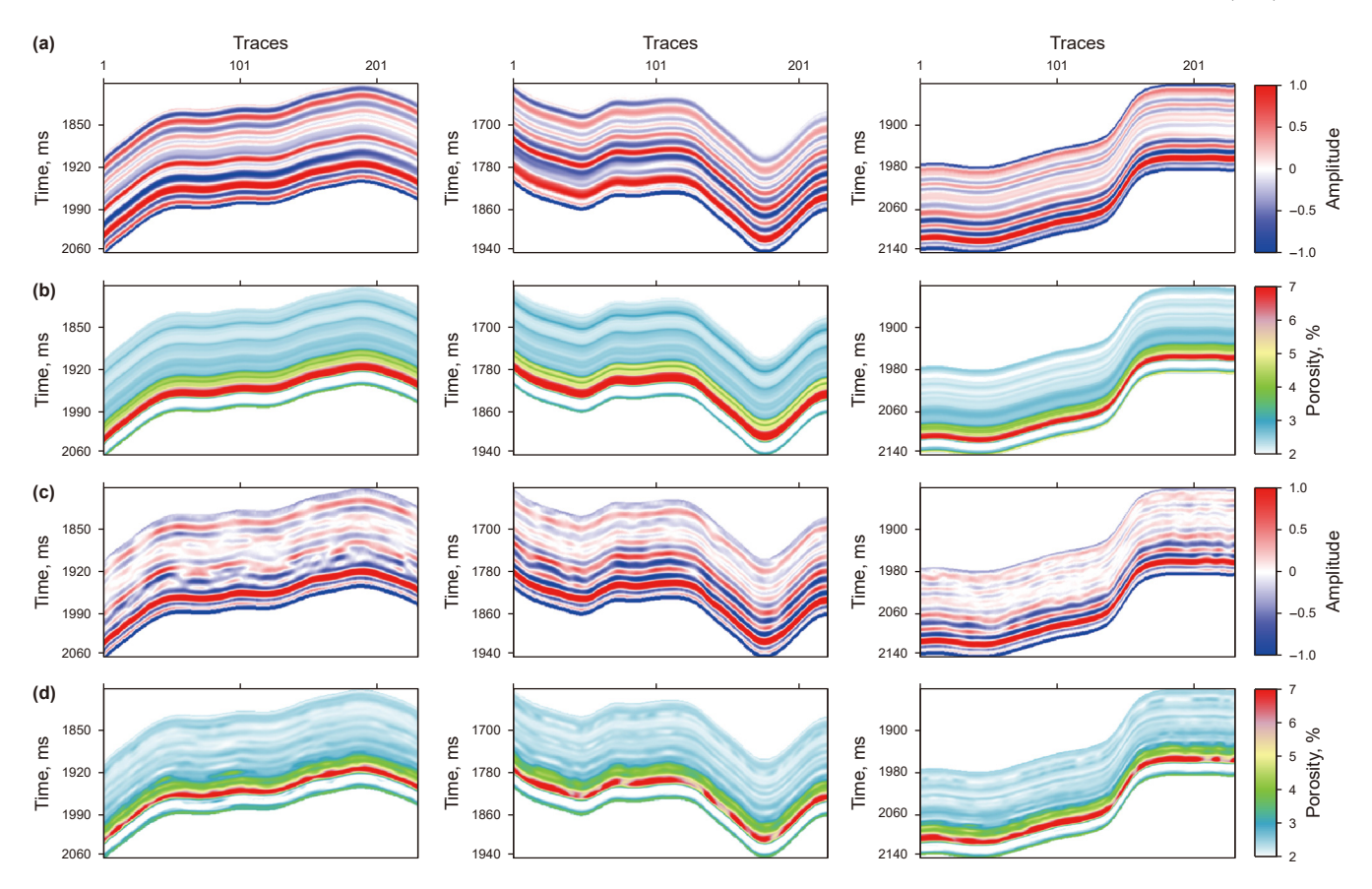
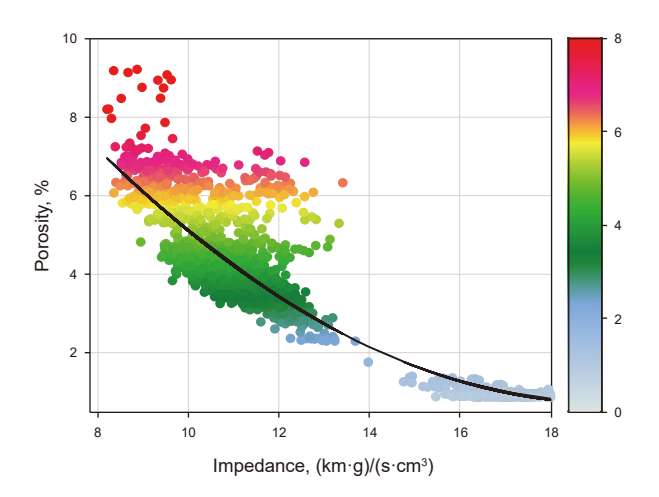


Fig. 14. Modeling results of study area B. The SM method constructed (a) seismic and (b) porosity dataset. The ISM constructed (c) seismic and (d) porosity dataset. Each column result from the same profile data.



**Fig. 15.** Petrophysical crossplot between porosity and impedance of well log data in study area B, the formula of the black fitting line is  $\phi=0.0731Z_p^2-2.5795Z_p+23.6868$ , and the color of each point denotes its porosity value.

predictions. The petrophysical property information identified at the B2 well indicated by the blue arrow is consistent with the well logs. Furthermore, Fig. 17(d)—(f) show the forward residual of the predicted porosity. The one-dimensional algorithm is difficult to adapt to discontinuous undulating structures, so the residual is relatively large; the conventional two-dimensional algorithm

considers the lateral continuity of seismic data, and the forward residual is sharply reduced; on this basis, the ISM learning with waveform constraints effectively considers the spatial variability of the strata, and the residual is further suppressed. This reflects the technical adaptability and superiority of ISM learning for interpreting complex and discontinuous reflection strata.

We further extract the predicted porosity using different methods for the B1 and B2 wells, and quantitatively evaluate the correlation and relative error with the logging porosity, as shown in Fig. 18 and Table 2. Compared with two-dimensional algorithms, 1D learning has a larger overall deviation, which is also confirmed by the mean square error in Table 2. The overall correlation of SM learning has been improved to a certain extent, but there is a significant deviation in the prediction performance at favorable reservoirs in well B2, as indicated by the blue arrow in Fig. 18(b). This also indicates that the method needs further optimization in the fineness of modeled sample set. The consistency between the prediction results of well nearby trace extracted by ISM learning and the logging porosity is the best. In addition, the PCC and MSE indicators also confirm that the performance of this method is quantitatively optimal, reaching 0.9415 and 0.9322, as well as 0.0029 and 0.0079, respectively, in well B1 and B2, leading the comparison method. This can demonstrate the applicability and effectiveness of the proposed ISM learning method in unconventional shale study area B. The porosity prediction results based on this method can further explain favorable areas and guide well deployment.

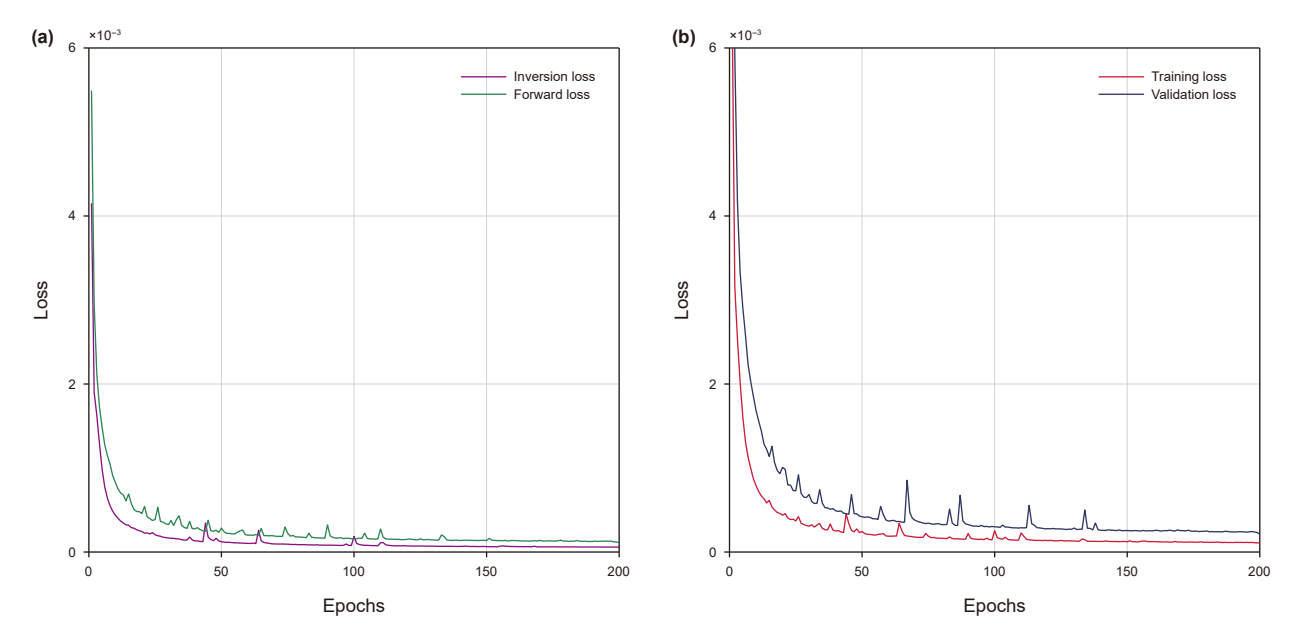


Fig. 16. Training loss of dataset from study area B. (a) Separate network loss, and (b) training and validation loss.

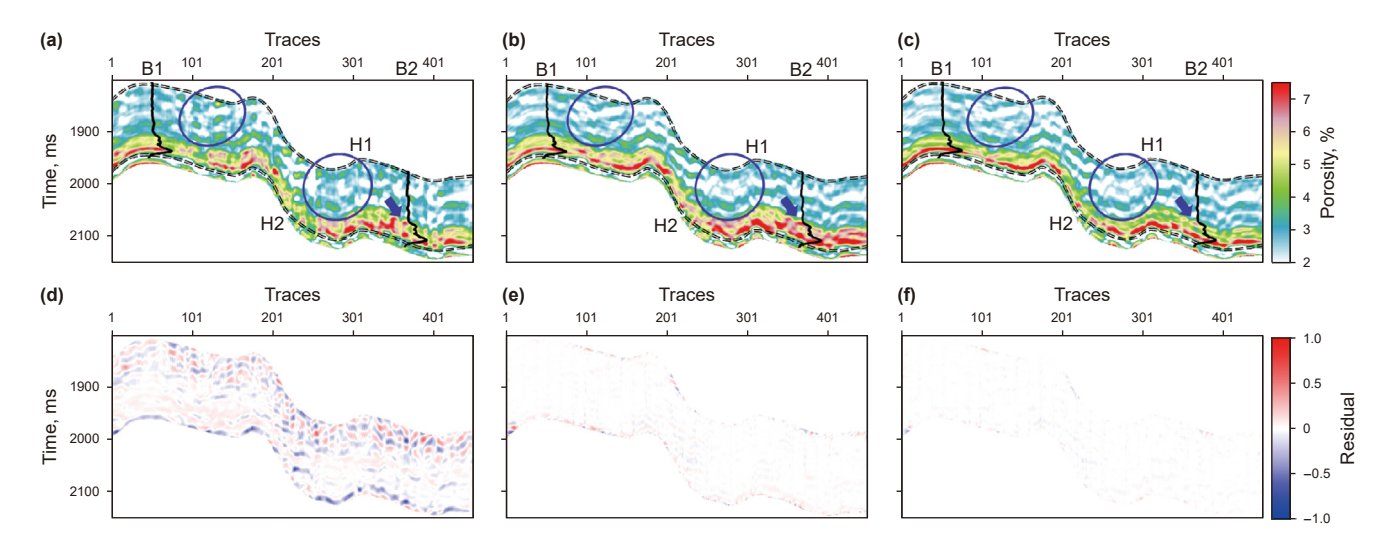


Fig. 17. Prediction results of seismic data cross wells B1 and B2 in study area B based on different methods. Predicted porosity of (a) 1D learning, (b) SM learning and (c) ISM learning, the projected black curves represent logging porosity. The residual between real seismic data and synthetic seismic data of (d) 1D learning, (e) SM learning and (f) ISM learning.

# 4. Conclusion

We propose a porosity prediction method based on ISM learning to enable intelligent and fine prediction of reservoir properties in structurally complex and well limited study areas. We use seismic waveforms, horizons, and well data to jointly construct a dataset with sedimentary facies-controlled significance, which effectively considers the lateral continuity and variability of seismic data and increases the adaptability to complex structures. In order to break through the bottleneck of small sample, we introduce the gated axial attention mechanism and design an improved inversion-forward bidirectional closed-loop network system, which makes the proposed method highly adaptable to few wells study areas. In addition, we introduce petrophysical information as guidance and

construct an adaptive weight coefficient using the inherent physical correlation between impedance and porosity. Numerical tests have confirmed that adaptive weight coefficient improves the accuracy of predicted porosity, and it is conductive for network to capture a more accurate elastic-petrophysical property mapping relationship. Finally, we present the examples of a buried hill study area and an unconventional shale study area. Compared to conventional one-dimensional deep learning method and SM deep learning method, the proposed ISM learning algorithm improves the accuracy and lateral continuity of predicted porosity, achieving better alignment with logging porosity. These results highlight the promising application potential of ISM learning method in complex reservoir prediction.

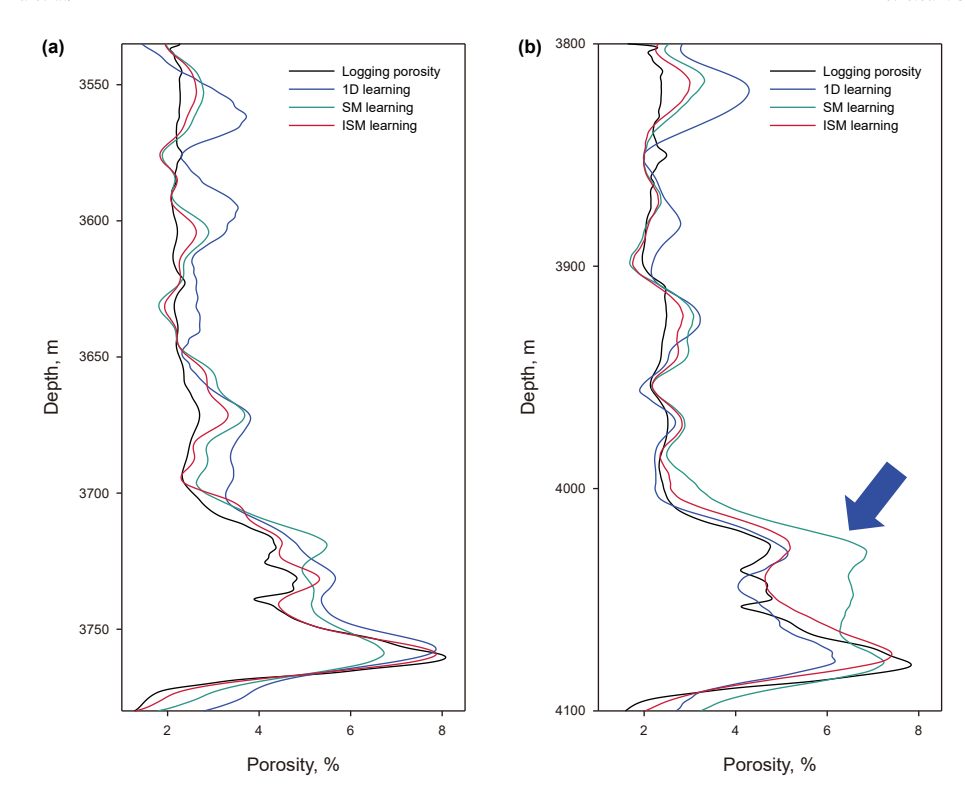


Fig. 18. Comparison of the prediction results at the location of the (a) well B1 and (b) well B2.

**Table 2** Prediction performance of wells B1 and B2.

Metrics	Well B1			Well B2		
	1D	SM	ISM	1D	SM	ISM
PCC MSE	0.9071 0.0178	0.9137 0.0105	0.9415 0.0029	0.8889 0.0202	0.8916 0.0283	0.9322 0.0079

### **CRediT authorship contribution statement**

**Bo-Cheng Tao:** Writing — original draft, Visualization, Validation, Software, Methodology, Investigation, Conceptualization. **Huai-Lai Zhou:** Supervision, Resources, Project administration, Funding acquisition, Conceptualization. **Wen-Yue Wu:** Data curation. **Gan Zhang:** Data curation. **Bing Liu:** Validation, Formal analysis. **Xing-Ye Liu:** Writing — original draft, Validation, Conceptualization.

# **Declaration of competing interest**

The authors declare that they have no known competing financial interests or personal relationships that could have appeared to influence the work reported in this paper.

#### Acknowledgments

The authors declare that no AI or AI-assisted technology was used in the writing process of this work. We greatly appreciate the support of Research Program of Fine Exploration and Surrounding Rock Classification Technology for Deep Buried Long Tunnels Driven by Horizontal Directional Drilling and Magnetotelluric Methods Based on Deep Learning under Grant E202408010, and the Sichuan Science and Technology Program under Grant 2024NSFSC1984 and Grant 2024NSFSC1990.

#### References

Adelinet, M., Ravalec, M., 2015. Effective medium modeling: how to efficiently infer porosity from seismic data? Interpretation 3 (4), SAC1—SAC7. https://doi.org/10.1190/INT-2015-0065.1.

Aki, K., Richards, P.G., 2002. Quantitative Seismology. University Science Books.

Aleardi, M., Ciabarri, F., Gukov, T., 2018. A two-step inversion approach for seismicreservoir characterization and a comparison with a single-loop Markov-chain Monte Carlo algorithm. Geophysics 83 (3), R227–R244. https://doi.org/10.1190/ geo2017-03871

Alfarraj, M., AlRegib, G., 2019. Semi-supervised sequence modeling for elastic impedance inversion. Interpretation 7 (3), SE237–SE249. https://doi.org/ 10.1190/INT-2018-0250.1.

Ali, A., Azeem, T., Khalid, R.F., et al., 2023. Delineation of thin-bedded sands and porosity using post-stack seismic inversion in the Lower Goru Formation, Kadanwari gas field, Pakistan. J. Earth Syst. Sci. 132 (60). https://doi.org/10.1007/ s12040-023-02071-8.

Avseth, P., Mukerji, T., Mavko, G., 2010. Quantitative Seismic Interpretation: Applying Rock Physics Tools to Reduce Interpretation Risk. Cambridge University Press, Cambridge, UK.

Bernabé, Y., 1995. The transport properties of networks of cracks and pores. J. Geophys. Res. Solid Earth 100 (B3), 4231–4241. https://doi.org/10.1029/94IB02986.

Bosch, M., 2004. The optimization approach to lithological tomography: combining seismic data and petrophysics for porosity prediction. Geophysics 69 (5), 1272–1282. https://doi.org/10.1190/1.1801944.

Chen, J., Liu, Y., Yu, Q., et al., 2021. TransUNet: Transformers Make Strong Encoders for Medical Image Segmentation, arXiv:2102.04306.

Chen, T., Wang, Y., Li, K., et al., 2023. A prestack seismic inversion method constrained by facies - controlled sedimentary structural features. Geophysics 88 (2), R209–R223. https://doi.org/10.1190/geo2022-0301.1.

Chen, Y., Bi, J., Qiu, X., et al., 2020. A method of seismic meme inversion and its application. Petrol. Explor. Dev. 47 (6), 1149–1158. https://doi.org/10.11698/PED 2020.06.08

Das, V., Mukerji, T., 2020. Petrophysical properties prediction from prestack seismic data using convolutional neural networks. Geophysics 85 (5), N41–N55. https://doi.org/10.1190/geo2019-0650.1.

Das, V., Pollack, A., Wollner, U., et al., 2019. Convolutional neural network for seismic impedance inversion. Geophysics 84 (6), R869—R880. https://doi.org/ 10.1190/geo2018-0838.1.

Doyen, P.M., 1988. Porosity from seismic data: a geostatistical approach. Geophysics 53 (10), 1263–1275. https://doi.org/10.1190/1.1442404.

Fattahi, H., Karimpouli, S., 2016. Prediction of porosity and water saturation using pre-stack seismic attributes: a comparison of Bayesian inversion and computational intelligence methods. Comput. Geosci. 20, 1075—1094. https://doi.org/

#### 10.1007/s10596-016-9577-0.

- Feng, R., Hansen, T., Grana, D., et al., 2020. An unsupervised deep-learning method for porosity estimation based on poststack seismic data. Geophysics 85 (6), M97—M105. https://doi.org/10.1190/geo2020-0121.1.
- Figueiredo, L., Grana, D., Roisenberg, M., et al., 2019. Gaussian mixture Markov chain Monte Carlo method for linear seismic inversion. Geophysics 84 (3), R463–R476. https://doi.org/10.1190/geo2018-0529.1.
- Figueiredo, L., Grana, D., Santos, M., et al., 2017. Bayesian seismic inversion based on rock-physics prior modeling for the joint estimation of acoustic impedance, porosity and lithofacies. J. Comput. Phys. 336, 128–142. https://doi.org/10.1016/ i.icp.2017.02.013.
- Gholami, A., Amirpour, M., Ansari, H.R., et al., 2022. Porosity prediction from prestack seismic data via committee machine with optimized parameters. J. Pet. Sci. Eng. 210. https://doi.org/10.1016/j.petrol.2021.110067.
- Han, H., Liu, H., Sang, W., et al., 2022. Seismic and well logs integration for reservoir lateral porosity prediction based on semi supervised learning. Chin. J. Geophys. 65 (10), 4073–4086. https://doi.org/10.6038/cjg2022P0410.
- Helgesen, J., Magnus, I., Proser, S., et al., 2000. Comparison of constrained sparse spike and stochastic inversion for porosity prediction at Kristin field. Lead. Edge 19, 400–407. https://doi.org/10.1190/1.1438620.
- Huang, X., Li, L., Li, F., et al., 2020. Development and application of iterative facies-constrained seismic inversion. Appl. Geophys. 17 (4), 522–532. https://doi.org/10.1007/s11770-020-0837-3.
- Jin, H., Liu, C., Guo, Z., 2024. Estimating pore pressure in tight sandstone gas reservoirs: a comprehensive approach integrating rock physics models and deep neural networks. J. Appl. Geophys. 230. https://doi.org/10.1016/j.jappgeo.2024.105526.
- Johansen, T.A., Jensen, E.H., Mavko, G., et al., 2013. Inverse rock physics modeling for reservoir quality prediction. Geophysics 78 (2), M1–M18. https://doi.org/ 10.1190/geo2012-0215.1.
- Lindseth, R.O., 1979. Synthetic sonic logs—a process for stratigraphic interpretation. Geophysics 44 (1), 3–26. https://doi.org/10.1190/1.1440922.
- Liu, M., Yao, D., Guo, J., et al., 2022. Reservoir porosity prediction model based on improved shuffled frog leaping algorithm and BP neural network. In: 2022 7th International Conference on Cloud Computing and Big Data Analytics, Chengdu, China. https://doi.org/10.1109/ICCCBDA55098.2022.9778868.
- Liu, T., Ma, Z., Wang, J., et al., 2015. Integrating MDT, NMR log and conventional logs for one-well evaluation. J. Pet. Sci. Eng. 46, 73–80. https://doi.org/10.1016/ j.petrol.2004.09.001.
- Liu, X., Chen, X., Cheng, J., et al., 2023a. Simulation of complex geological architectures based on multistage generative adversarial networks integrating with attention mechanism and spectral normalization. IEEE Trans. Geosci. Rem. Sens. 61. https://doi.org/10.1109/TGRS.2023.3294493.
- Liu, X., Chen, X., Li, J., et al., 2020. Facies identification based on multikernel relevance vector machine. IEEE Trans. Geosci. Rem. Sens. 58, 7269–7282. https://doi.org/10.1109/TGRS.2020.2981687.
- Liu, X., Cheng, J., Cai, Y., et al., 2022. Stochastic simulation of facies using deep convolutional generative adversarial network and image quilting. Mar. Petrol. Geol. 146. https://doi.org/10.1016/j.marpetgeo.2022.105932.
- Liu, X., Shao, G., Yuan, C., et al., 2022. Mixture of relevance vector regression experts for reservoir properties prediction. J. Pet. Sci. Eng. 214 (1). https://doi.org/10.1016/j.petrol.2022.110498.
- Liu, X., Wu, B., Yang, H., 2023b. Multitask full attention U-Net for prestack seismic inversion. IEEE Trans. Geosci. Remote Sens. Lett 20. https://doi.org/10.1109/ LGRS.2023.3303698.
- Liu, X., Zhou, H., Guo, K., et al., 2023c. Quantitative characterization of shale gas reservoir properties based on BiLSTM with attention mechanism. Geosci. Front. 14 (4). https://doi.org/10.1016/j.gsf.2023.101567.
- Luffel, D.L., Guidry, F.K., 1992. New core analysis methods for measuring reservoir rock properties of Devonian shale. J. Petrol. Technol. 44 (11), 1184–1190. https:// doi.org/10.2118/20571-PA.
- Misra, D., 2019. A self-regularized non-monotonic neural activation function. arXiv:, 1908.08681.
- Mukerji, T., Avseth, P., Mavko, G., et al., 2001a. Statistical rock physics: combining rock physics, information theory, and geostatistics to reduce uncertainty in seismic reservoir characterization. Lead. Edge 20, 313–319. https://doi.org/ 10.1190/1.1438938.
- Mukerji, T., Jørstad, P., Avseth, G., et al., 2001b. Mapping lithofacies and pore-fluid probabilities in North Sea Reservoir: seismic inversions and statistical rock

- physics. Geophysics 66 (6), 988-1001. https://doi.org/10.1190/1.1487078.
- Pang, M., Ba, J., Fu, L., et al., 2020. Estimation of microfracture porosity in deep carbonate reservoirs based on 3D rock-physics templates. Interpretation 8 (4), SP43—SP52. https://doi.org/10.1190/INT-2019-0258.1.
- Russell, B.H., 1988. Introduction to Seismic Inversion Methods. SEG.
- Sang, W., Yuan, S., Han, H., et al., 2023. Porosity prediction using semi-supervised learning with biased well log data for improving estimation accuracy and reducing prediction uncertainty. Geophys. J. Int. 232, 940–957. https://doi.org/10.1093/gji/ggac371.
- Shahraeeni, M.S., Curtis, A., Chao, G., 2012. Fast probabilistic petrophysical mapping of reservoirs from 3D seismic data. Geophysics 77 (3), O1–O19. https://doi.org/10.1190/geo2011-0340.1.
- Song, J., Ntibahanana, M., Luemba, M., et al., 2023. Ensemble deep learning-based porosity inversion from seismic attributes. IEEE Access 11, 8761–8772. https://doi.org/10.1109/ACCESS.2023.3239688.
- Su, Z., Cao, J., Xiang, T., et al., 2023. Seismic prediction of porosity in tight reservoirs based on transformer. Front. Earth Sci. 11. https://doi.org/10.3389/ feart.2023.1137645.
- Sun, J., Innanen, K.A., Huang, C., 2019. Physics-guided deep learning for seismic inversion with hybrid training and uncertainty analysis. Geophysics 86 (3), R303–R317. https://doi.org/10.1190/geo2020-0312.1.
- Tao, B., Liu, X., Zhou, H., et al., 2024. Porosity prediction based on a structural modeling deep-learning method. Geophysics 89 (6), M197–M210. https:// doi.org/10.1190/GE02024-0035.1.
- Valanarasu, J., Oza, P., Hacihaliloglu, I., et al., 2021. Medical Transformer: Gated Axial-Attention for Medical Image Segmentation. arXiv: 2102.10662.
- Vaswani, A., Shazeer, N., Parmar, N., et al., 2017. Attention is all you need. arXiv: 1706.03762
- Wong, P.M., Gedeon, T.D., Taggart, I.J., 1995. An improved technique in porosity prediction: a neural network approach. IEEE Trans. Geosci. Rem. Sens. 33 (4), 971–980. https://doi.org/10.1109/36.406683.
- Wu, X., Yan, S., Bi, Z., et al., 2021. Deep learning for multidimensional seismic impedance inversion. Geophysics 86 (5), R735–R745. https://doi.org/10.1190/ geo2020-0564.1
- Wyllie, M.R.J., Gregory, A.R., Gardner, L.W., 1956. Elastic wave velocities in heterogeneous and porous media. Geophysics 21 (1), 41–70. https://doi.org/10.1190/1.1438217.
- Yang, L., Wang, S., Chen, X., et al., 2023. High-fidelity permeability and porosity prediction using deep learning with the self-attention mechanism. IEEE Transact. Neural Networks Learn. Syst. 34 (7), 3429–3443. https://doi.org/ 10.1109/TNNLS.2022.3157765.
- Yang, N., Li, G., Zhao, P., et al., 2023. Porosity prediction from pre-stack seismic data via a data-driven approach. J. Appl. Geophys. 211. https://doi.org/10.1016/ j.jappgeo.2023.104947.
- Yuan, S., Jiao, X., Luo, Y., et al., 2022. Double-scale supervised inversion with a datadriven forward model for low-frequency impedance recovery. Geophysics 87 (2), R165—R181. https://doi.org/10.1190/geo2020-0421.1.
- Yuan, S., Wang, S., Luo, C., et al., 2015. Simultaneous multitrace impedance inversion with transform-domain sparsity promotion. Geophysics 80 (2), R71–R80. https://doi.org/10.1190/geo2014-0065.1.
- Zhang, J., Sun, H., Zhang, G., et al., 2022. Deep learning seismic inversion based on prestack waveform datasets. IEEE Trans. Geosci. Rem. Sens. 60. https://doi.org/ 10.1109/TGRS.2022.3195858.
- Zhang, S., Huang, H., Li, H., et al., 2017. Prestack seismic facies-controlled joint inversion of reservoir elastic and petrophysical parameters for sweet spot prediction. Energy Explor. Exploit. 35 (6), 767–791. https://doi.org/10.1177/ 0144598717716286
- Zhang, X., Guo, Z., Liu, C., 2024. Characterization of horizontal fractures in shale gas reservoirs using a rock-physics-based method integrated with SA-PSO algorithm and CNN. IEEE Trans. Geosci. Rem. Sens. 62, 1–14. https://doi.org/10.1109/TCPS-2024.477057
- Zheng, Z., Pan, S., Luo, H., et al., 2020. Porosity prediction based on gs+ga-XGBoost. 2020 IEEE intl conf on parallel & distributed processing with applications, Big data & cloud computing. Sustainable Computing & Communications, Social Computing & Networking, Exeter, United Kingdom 1014—1020. https://doi.org/ 10.1109/ISPA-BDCloud-SocialCom-SustainCom51426.2020.00153.
- Zou, C., Zhao, L., Xu, M., et al., 2021. Porosity prediction with uncertainty quantification from multiple seismic attributes using random forest. J. Geophys. Res. Solid Earth 126. https://doi.org/10.1029/2021JB021826.